Coatings for Decarburization Prevention and The Influence of Electromagnetic Field on Carbon Diffusion in Iron

BY

JIAWEI HU

Institut National des Sciences Appliquées

21/02/2019

Work performed at: MATEIS
Under the supervision of: Patrice Chantrenne

Contents

1. Introduction

The main goal of this project is to analyze experimentally the influence of a combination of electric and magnetic field on the diffusion process of carbon atoms in iron. The behavior of carbon atoms under either electric or magnetic field has yet been studied separately, but not a combination of both.

Take electromigration as an example, the presence of an electric field can cause gradual movements of ions in a conductor due to the momentum exchange of the flowing electrons with diffusion metal atoms. The electrostatic force in an electric field causes the electrons to move in the opposite direction as the electric field, and electromigration takes place when some of the momentum is transferred from the charge carrier to a nearby ion, causing it to move from its original position. This process is multiplied over time and can lead to creating gaps in the conducting metal, preventing its current conduction.

Chantrenne et al. [1] have shown that the carbon diffusion depth in iron in the $\alpha+\gamma$ region can be enhanced with the presence of an electric field when the direction of the diffusion and the electric field are parallel, and the phenomenon is reduced when these directions are antiparallel.

When it comes to the influence of magnetic fields, as shown by Shou-Jing Wang et al. [2], the presence of magnetic field slightly promotes the carbon diffusion in γ-Fe in the direction parallel/antiparallel to the magnetic field, and it hinders the carbon diffusion in the direction perpendicular to the magnetic field direction.

The goal of this project is to study the influence of a combination of both phenomena.

In our experiment, a pure iron sample (99,99%) with a 26mm x 9 mm dimension and partly covered by graphite glue is put into the oven to start the process, the chamber operates in a near vacuum environment at around 900ºC for 7 hours and it is submitted under both electrical and magnetic fields.

In order to better analyze the diffusion process under the above-described circumstances, optical microscopy is set to record the changes of the microstructure.

The decarburization process which would inevitably take place in the exposed area of the sample during the experiment is undesired owing to the fact that it disturbs the results, hence a coating with decarburization prevention function is required for the success of this experiment. In an optimal scenario, this coating must be inert with carbon and iron, able to prevent decarburization, stable under the described thermal environment and transparent so the optical observation during the experiment can still take place.

The first part of the project is devoted to finding the proper coating to prevent decarburization for the treated sample.

2. Experimental

2.1. Approaches to the problem

Three different approaches are taken to obtain coatings that meet the requirements:

1. Literature research. Look for studies that are done previously to prevent decarburization phenomenon, in industrial or academic domains.

2. Experimental tryout.

    a. Test with the coatings available in Lyon Institute of Nanotechnology:
    Sputtering for Al_2O_3 coating.
    Vaporization for Au coating.
    TiN, TiO_2, CrN, Cr_2O_3.
    Coatings from few nm to 800-900nm: Pd, Ag, Pt, Ge, SiO_2.
    Coatings of 2 to 3µm: Pd, Ag.

    b. BN Spray.

3. Usage of Thermo-Calc. Use this software that runs simulations based on databases to find proper elements that do not mix with carbon nor iron in thermodynamic equilibrium conditions.

The preparation of the sample prior to the coating involves two steps: surface polishing and the application of graphite glue to provide carbon. Previous experiments have shown that, for the employed material, a smooth surface is required for the carbon atoms from the graphite glue to diffuse into the iron.

The iron sample is first cut to obtain the desired dimension (26mm x 9mm x 1mm) and later polished to obtain smooth surfaces. Abrasive papers with grit sizes from P80 to P2400 were used, as well as solutions of alumina particles of 3µm and 1µm. In order to prevent oxidation, following each polishing, the polished surface must be rinsed with ethanol and dried. An illustration of the sample is demonstrated in Fig. 1. Graphite glue is then applied on both surfaces and let to dry for several hours.

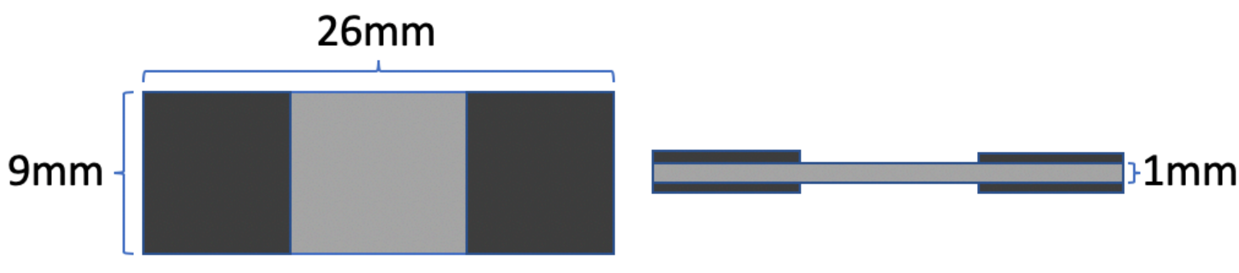

Fig. 1. Illustrations of the employed sample. The geometry of the sample is 26x9x, with graphite glue applied on the two extremes.

The illustrated graphite glue application is designed to better visualize the effects of either electric or electric and magnetic field on carbon diffusion. With an electric field pointing from one side to another side of the sample, this arrangement would allow having two carbon diffusion directions that are in parallel and antiparallel with electric field respectively. Consequently, the comparison of the results could be done within a single specimen.

2.2. Coating reliability testing

When a coating is being selected and applied with its due preparation process, the reliability of the obtained coating-sample system must be examined.

Two different methods were employed with this purpose:

1. Secondary-vacuum oven. The oven is assisted by two pumps to obtain the vacuum level. The sample is put into a glass tube which in turn is inserted into the oven that operated at 875ºC for 7h. After the heating the sample is let to cool down in the oven. The heating rate is 30ºC/mins. A low-pressure level is required in order to keep oxidation out of equation.

2. Furnace with electric field. An illustration of the setup is shown in Fig. 2. The sample is placed between two electrodes to provide bias and electric current would pass through the sample. An upper pressing piece and graphite sheets are used to increase contact when closing the furnace. A set of thermocouples is to be welded to the sample, in the middle of the sample close to the edge, in order to determine its temperature during the experiment.

   The heating would start by the Joule effect from the sample when a 14A current flows through, later the inner resistance of the furnace would provide extra heating for the sample to reach a temperature about 875ºC for 6 to 7 hours. The bias between the electrodes when the temperature of the sample reaches its steady state is about 3 to 3,5V. The temperature of the system is controlled via a dynamic system controlling software and the time required to reach steady state is around 1h30mins.

   The furnace operates in the first-level vacuum and a cooling system is to protect the setup from overheating.

   Given the non-electrically-conducting nature of BN and alumina, the sample preparation process involving samples coated with these materials requires removing coatings on certain areas of the specimen so the current could flow through it. A sharp knife is used to scratch off part of the coating that covers the bottom surface of the sample that is in contact with graphite sheets. The area of the coating being removed should be minimized as long as the flow of electric current is detected by the system.

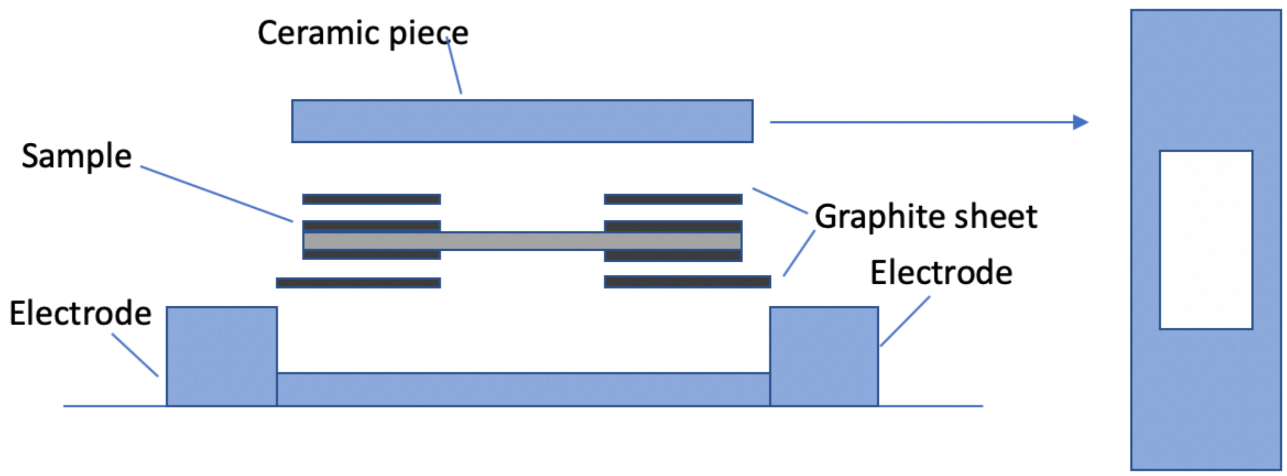

Fig. 2. Illustration of the furnace with electric field.

A metallographic analysis is carried out to examine whether the coating has the desired decarburization prevention ability. For this, the obtained piece is mounted with resin exposing its cross-section, later polished and chemically etched for microscopic observation. Microscopical images of the sample are also taken for image processing, *ImageJ*, an image processing software is employed to obtain phase percentage along its cross-section. The results may be plotted and compared among different samples.

The metric to be used to determine whether the employed coating is useful is then determining the diffusion length of the carbon atoms from the limit of graphite glue. If the sample has no protection or the coating is not as useful, the carbon diffusion depth would be held to zero. The length of the applied graphite glue at both surfaces of the sample should be previously measured and compared to the length of the region with pearlite.

An optical microscope is used to determine both the initial length of the graphite glue and the diffusion length of carbon atoms from the graphite-Fe interface.

Although the minimum unit of the XY Linear Transition Stage of the device is 0.001 inches (25.4 μm), the actual error that is being committed applying this method to compare the relative lengths could be more significant. The main reason being the irregularity of the edges of the glue and it makes it difficult to obtain a specific value. The error being committed when determining the length of graphite glue ranges between 0.005 and 0.01 inches, which are 127 and 254 μm respectively.

On the other hand, when the sample is being polished and prepared for microscopic observation, the actual amount of the material being eliminated is unknown since the sample is embedded in resin.

The theoretical carbon diffusion length, taking into account the phase transition phenomenon induced by carbon atoms in the given experimental conditions, is about several mm, the reason why, despite the increased error being committed, it is still a valid method to testify the decarburization-prevention ability of the coatings.

2.3. Cementation with electric and magnetic field

An 8T magnetic field is generated by a set of coils placed inside a container, cooled with liquid helium at 4K to obtain superconductivity.

The preparation for the experiment is similar to the previous one. When the specimen is placed in the experimental setup above-described, it is placed in the center of the coil for the cementation to take place under both electric and magnetic field. The direction of the magnetic field is perpendicular to the direction of diffusion and the electric field with the sense pointing downwards. The position of the sample inside the coil must be the one that matches with the neutral line of the field to secure a homogeneous distribution of the field line throughout the sample. This position for the employed system has a range of around 3 cm in the middle of the device. Fig. 3 illustrates the direction of the electric and magnetic field of the experiment.

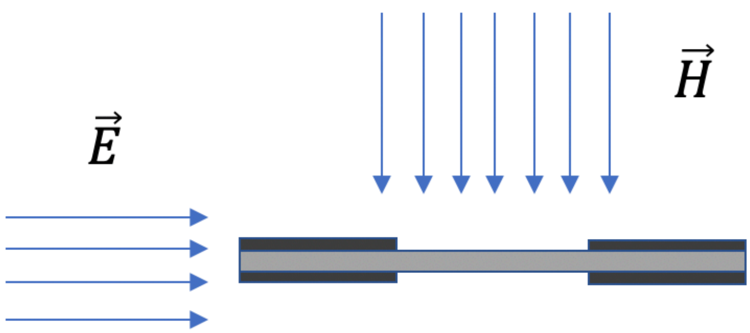

Fig. 3. Direction of the electric and magnetic field applied on the sample during cementation.

3. Results and Discussion

3.1. Results from the literature research

Two coatings were found during the literature research, both of them are ceramic coatings designed to protect steels from oxidation and decarburization during heat treatments in industrial scales and can be applied either by painting or spraying.

The first found coating consists of dolomite, bauxite and silicon carbide. The mixture is diluted with water to obtain the proper viscosity and the addition of citric acid as a binding agent was to secure a good adhesion to the surface of the steel after drying. In this study done by Xiaojing Wang *et al* [3], the coating was applied on bearing steels, and it was able to successfully prevent decarburization at 1250ºC for up to 2h.

The powder of the second coating is a mixture of bauxite, which provides mainly Al2O3 and SiO2, and SiC. It is mixed with sodium silicate dispersant and aluminum dihydrogen phosphate binder with a weight ratio of 10:5:1. Xiaojing Wang *et al* [4] applied the obtained slurry to coat the spring steel substrate. The coating reduced the decarburization effect by 71.84% at temperatures < 1050ºC, and the protective effect increases up to 100% for temperatures > 1050ºC for 60 min.

Two main concerns are involved when it comes to applying these coatings for the experiment. The first is the difference of the substrate used for our experiment and the ones used in these studies, this may play an important role when it comes to affecting the reliability of the coating. The temperature of the thermal treatment from the studies also differed from the ones of our interest. Both articles suggest that high temperature is a key factor for the compaction of the coating, its decarburization prevention effect can be reduced at a lower temperature.

Though the usage of these coatings still remains to be seen, mainly due to the complexity of obtaining the base materials to form the coating, one of the components has been consistent in terms of mass percentage in the composition of both found coatings, which is alumina. This provides with a strong motivation to used alumina as a coating for this process.

3.2. Results from the experimental tryout

3.2.1. Eliminated elements

The experiment requires the coating to be able to withstand the thermal conditions as well as to be inert with both carbon and iron. The coatings using elements that are not satisfying these conditions are eliminated from the experimental tryout.

As shown in Table 1. **Ge** and **Ag** are out of consideration due to their low fusion point, temperature of the experiment is about 900ºC.

	Ge	Ag	Pd	Pt
Fusion Point(ºC)	940	960	1555	1768

Table 1. Melting points(ºC) of Ge, Ag, Pd and Pt.

Pd and Pt are elements able to form alloys with Fe, as shown in Fig. 4 and 5, thus their elimination as elements for coating.

In the case of CrN, which can be formed by direct combination of Cr and N at 800ºC. W. Ernst *et al.* [5] reported that CrN coatings start to decompose above 925ºC under release of nitrogen in two major reaction steps to pure Cr via the intermediate step of Cr2N.

Materials such as TiO_2, TiN, SiO_2 and Cr_2O_3 are yet to be tried in this work.

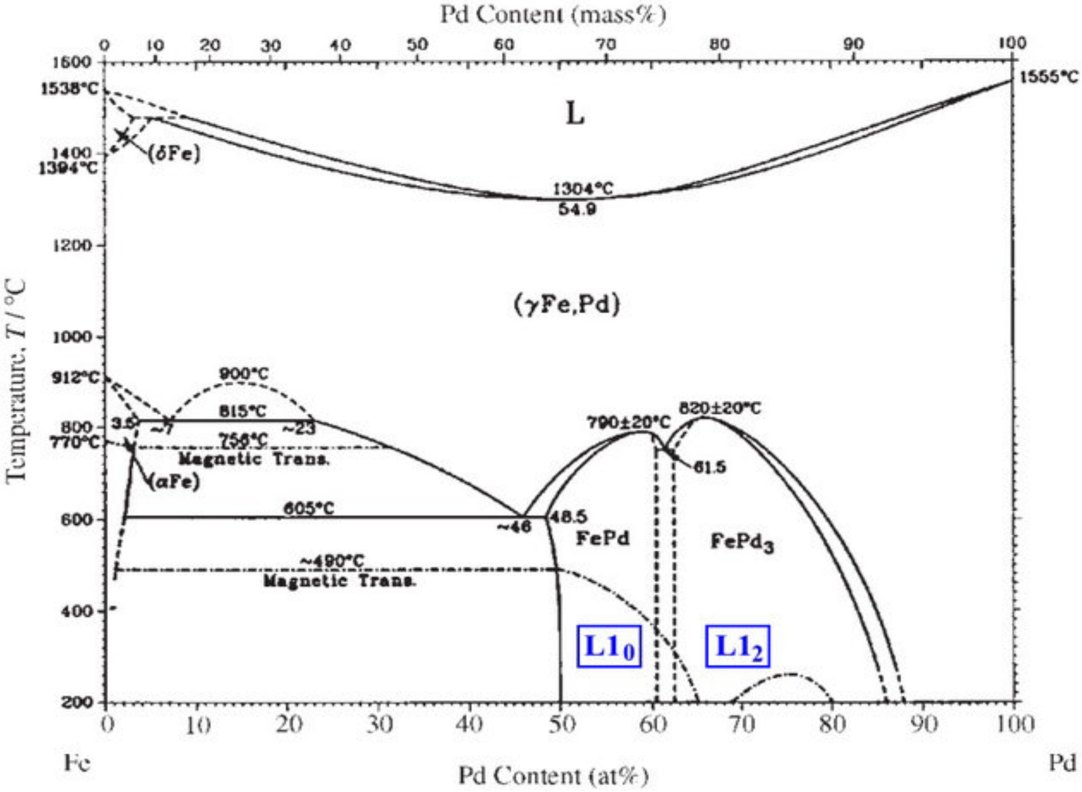

Fig 4. Pd-Fe Equilibrium phase diagram. [6]

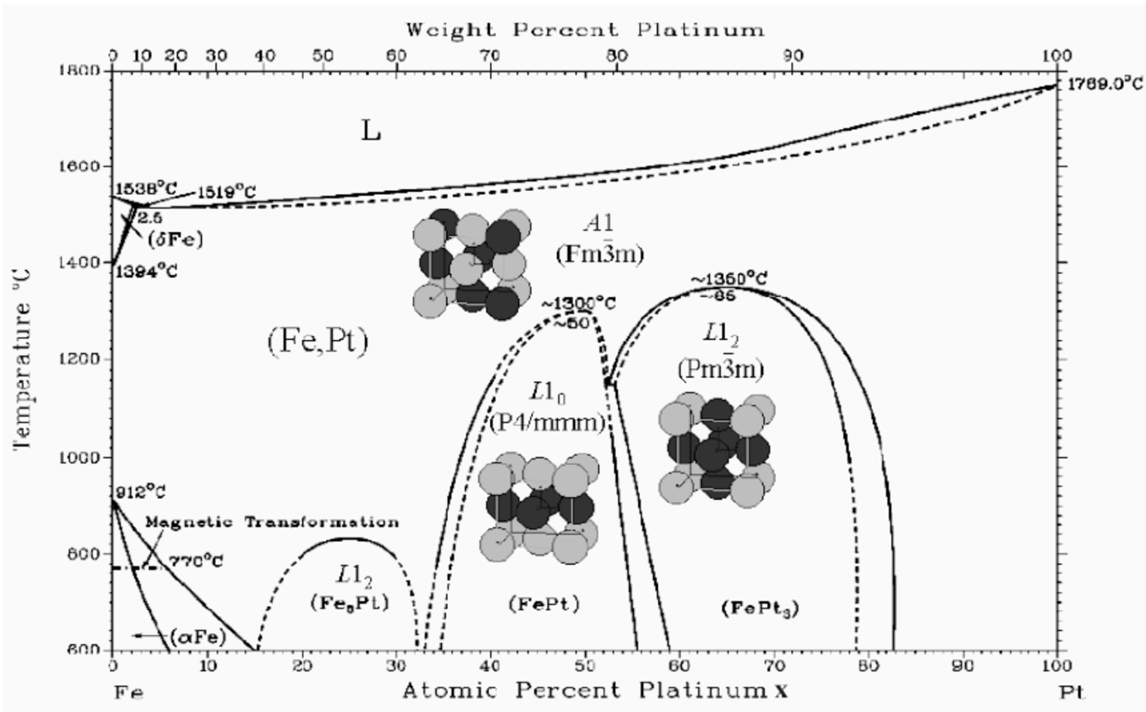

Fig 5. Fe-Pt Equilibrium phase diagram. [7]

3.2.2. Results from thermal treatment testing of the coatings

Tab.2 contains information regarding the samples used for experiments, its coating materials, thicknesses and the corresponding thermal treatment.

Sample	Coating	Thickness (nm)	Thermal treatment
NC	-	-	F*
Au1	Au	300	F
Au2			F + E**
Al1	Al_2O_3	240	F
Al2		980	F
Al3		240	F + E
Al4		980	F + E
BN1	BN	-	F
BN2			F + E
BN3			F + E + B***
BN4			F + E

Tab. 2. Information regarding coating, thickness and thermal treatment of different samples.
F, thermal treatment in conventional oven.*
*F+E**, thermal treatment with electric field.*
*F+E+B***, cementation with electric and magnetic field.*

3.2.2.1 Sample without coating

A sample with no coating (NC) is put into the vacuum assisted oven for thermal treatment.

The employed graphite glue after the thermal treatment became very fragile and a minimal movement can detach it from the surface with ease and turn it into dust.

Fig. 6a) shows the obtained microscopical image of the cross-section after metallographic preparations. The darker phase of pearlite, a laminar structure constituted by the alternating layers of ferrite and cementite, is appreciated in the area covered by graphite glue. Its distribution follows mostly along the grain limit of a more numerous ferrite phase, as shown in Fig. 6b).

A set of images were taken for image processing. The %pearlite of the sample along its cross-section is plot as a function of position, see Fig. 7. Images are taken along its cross-section from one extreme going inwards until the C-related phase disappears. In this case, 16 images were taken to cover the length of cross-section with pearlite presence, each image represents a small section of the cross-section, thus one “position”. An illustration relating the microscopical images and their position is shown in Fig. 8. As Fig. 7 displays, %pearlite increases from left to right reaching to its peak value around13% at about the middle and then it starts to decrease till zero. Assuming a homogeneous diffusion of carbon atoms from graphite glue to the sample, the graphic presents an expected result: %C is the highest in the middle of the graphite-glued area and its lowered as moving outwards. The decrease in %C is due to decarburization through the sample and/or its cross-section.

Although carbon diffusion is being observed within the sample with no coating, neither the amount of phase change nor its distribution is as expected for a sample that does not experience decarburization. In the case of obtaining a coating that prevents decarburization entirely, the sample would be expected to have a depth of carbon diffusion or phase change within the order of mm, considering a thermal treatment at 850ºC for 7h with neither electric nor magnetic field. On the other hand, even if it doesn’t invade the whole sample, the %pearlite should be higher on the edges than the center of the cross-section of the sample since diffusion happens inwards.

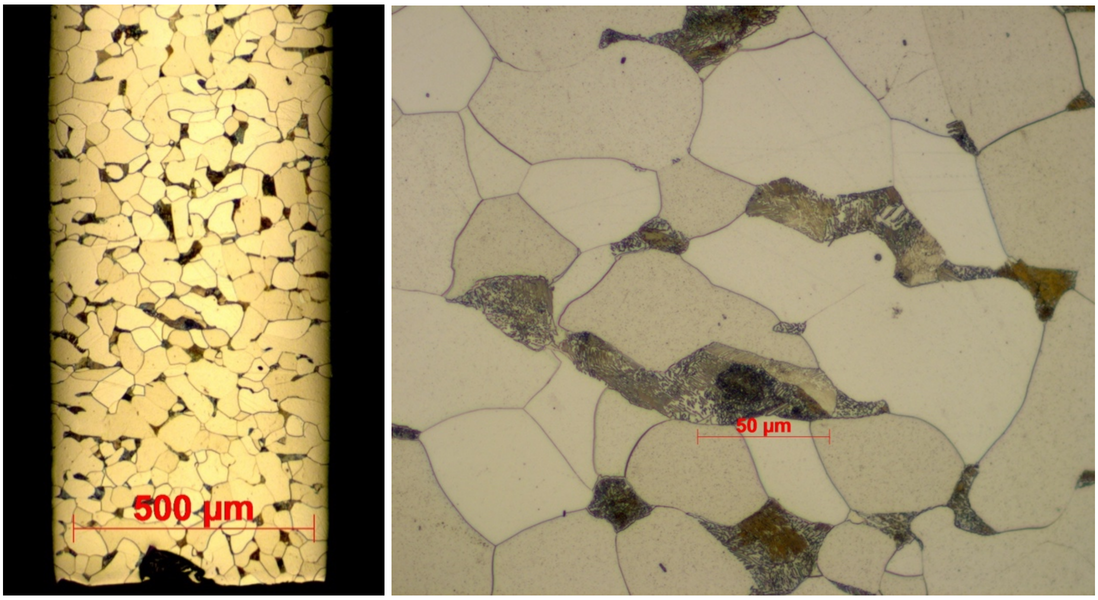

a) b)

Fig. 6. Microscopical image of the sample, areas covered by graphite glue. a) Magnification x5, b) distribution of pearlite along grain limits of ferrite, magnification x50.

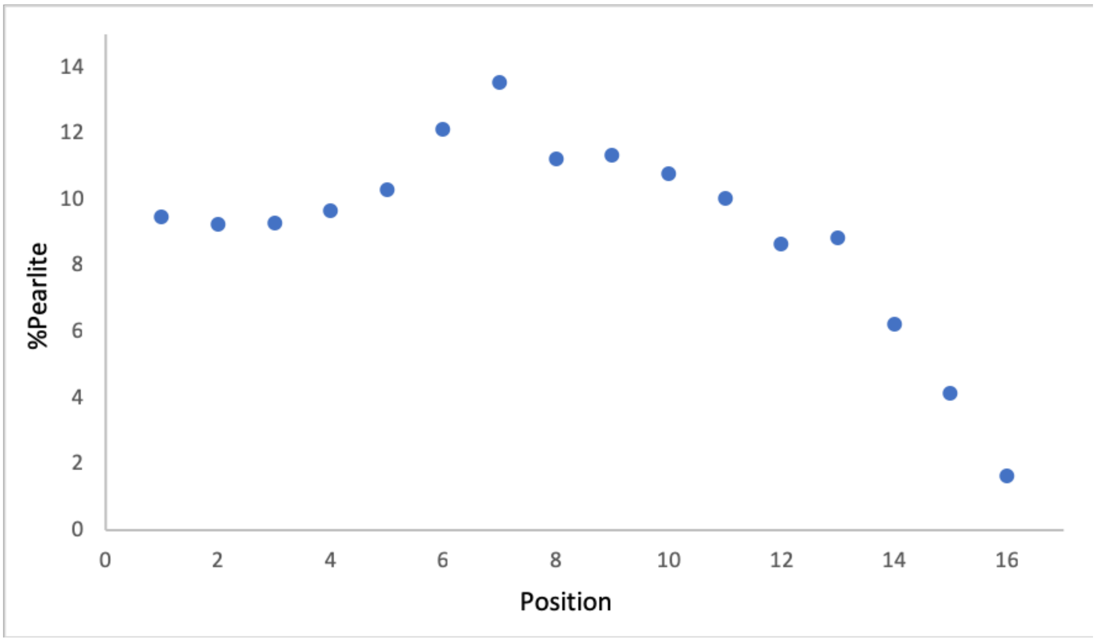

Fig. 7. %Pearlite of the sample along its cross-section vs. position from one extreme of the sample moving inward until the disappearance of C-related phase. 16 images were taken for this analysis.

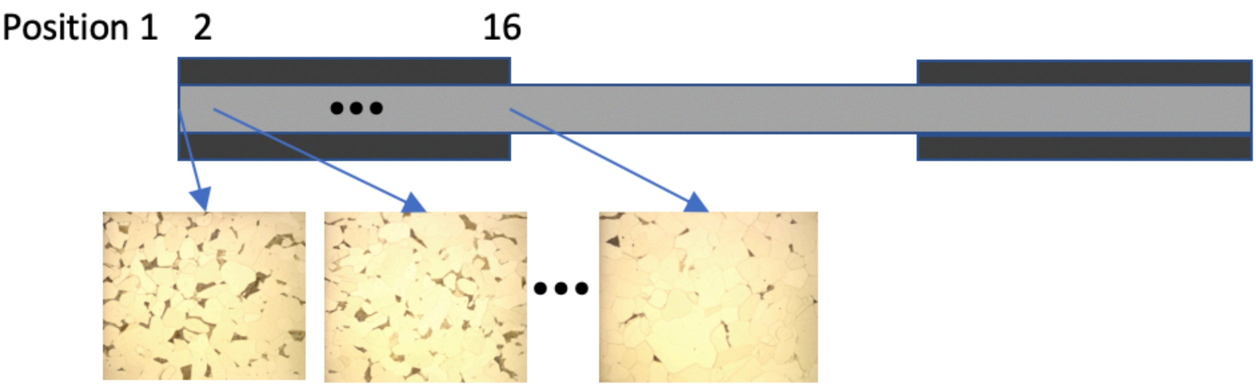

Fig. 8. Illustration for microscopical images relating to its corresponding positions.

3.2.2.2. Au coating

The application process involving gold deposition for this coating is called evaporation, a technique of thin-film deposition. Such a process is performed in vacuum, the target made of the element of interest is evaporated by a plasma and directly deposited and solidified on the sample, forming the coating.

Two Au-coated samples were tested and an image taken by SEM of the graphite-Fe interface is demonstrated in Fig. 9. In contrast with other samples, the graphite glue of the ones coated with Au is applied covering half surface of the sample.

Sample Au1 was tested in the vacuum-assisted thermal treatment at 875ºC for 8h. After the treatment, the presence of Au can only be visually appreciated on graphite glue as shown in Fig. 10. Carbon diffusion from graphite glue into the regions under it is observed in Fig. 11, similar to the case of sample NC, the amount of C diffusion is limited and no difference between the edge and the center of the sample is appreciated. Images along its cross-section were taken for %pearlite concentration analysis, as shown in Fig. 12, %pearlite reaches its peak value (21%) close to the middle and it decreases moving outwards. The C concentration decreases rapidly approaching the graphite-Fe interface due to decarburization.

Sample Au2 was tested in the oven with electric field. As in the previous case, the presence of gold can no longer be appreciated on the Fe surface after the treatment and only certain reduced areas on graphite glue had Au remaining on its surface, see Fig. 13.

Both surfaces were being prepared for microscopical observation and the presence of pearlite can only be observed under the areas with remaining Au coating. Fig. 14 shows the microscopical image of the area rich in carbon, an image analysis suggests that close to 45% of its area are pearlite.

Conclusions:

- The Au coating is poorly attached to the Fe surface, and a thermal treatment with electric current can affect its attachment to the graphite glue as well. Thin Au coatings tend to form nano-particles during heat treatment and it is not retained on the Fe surface afterward. Au coating sticks better on the surface of graphite glue but, according to the obtained results, the electric current cannot only inhibit carbon diffusion but also increase the chances for the Au-coating to be eliminated from the surface of graphite glue.

- Although C diffusion only occurred on a smaller area covered by graphite glue when it had thermal treatment with electric field, its C concentration is higher than when testing without.

- The comparison between graphite-glue length and the length of areas with pearlite phase was not done for Al1 since no measurements prior to the experiment were made. However, the diffusion profile of its cross-section and the way %pearlite is decreased approaching graphite-Fe interface in image analysis suggest that decarburization did indeed take place.

Fig. 9. Graphite-Fe interface of the Au coated sample with the dark area being the employed graphite glue. Image taken by SEM.

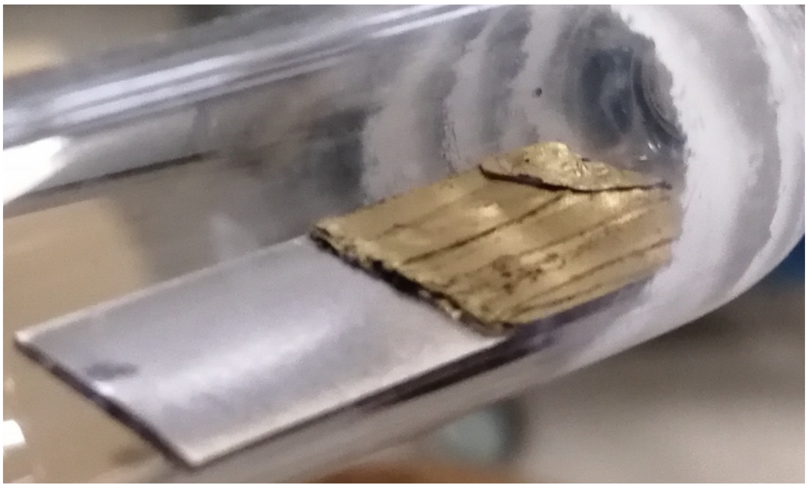

Fig. 10. Sample Au1 after thermal treatment, no coating on Fe surface is visually captured on Fe.

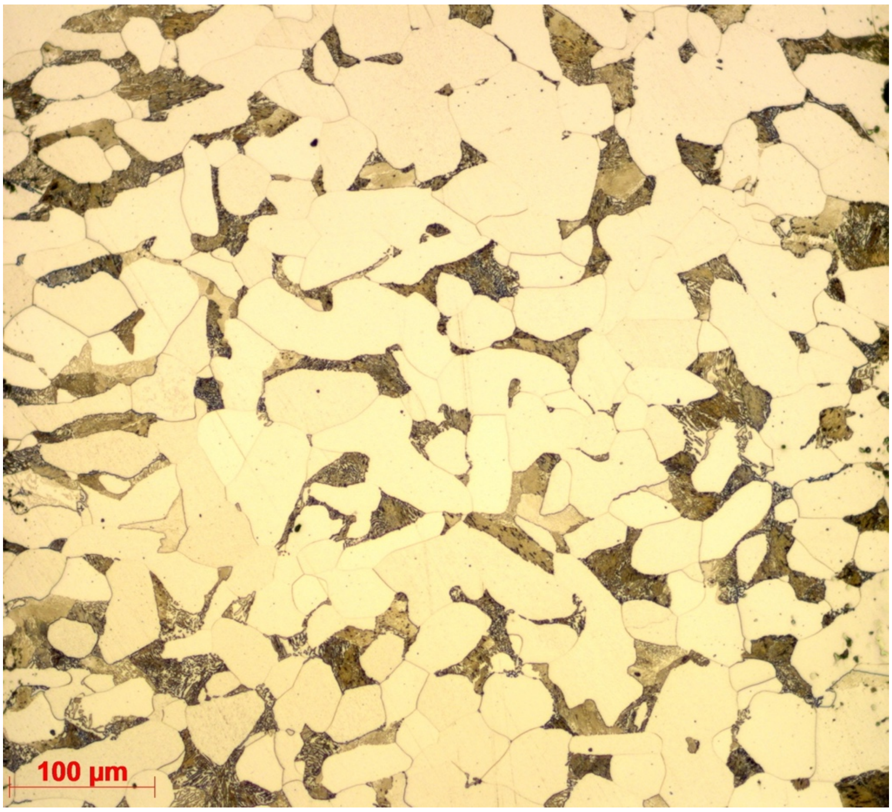

Fig. 11. Microscopic image of the area rich in C, sample Au1.

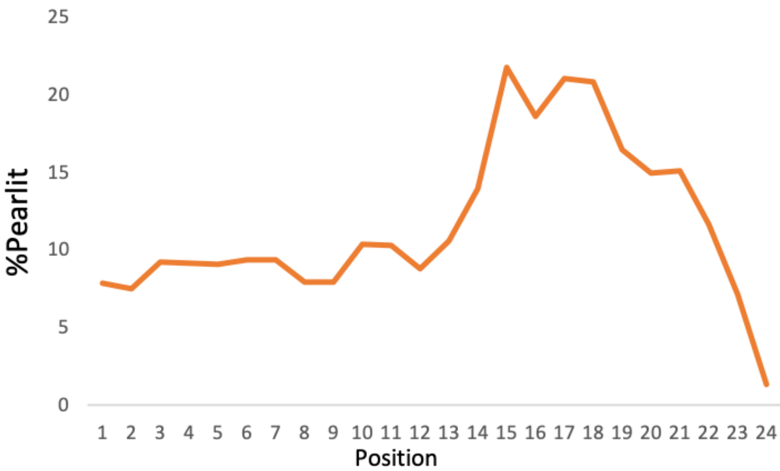

Fig. 12. Results of the image analysis of sample Au1. %pearlite of the cross-section vs. position from its edge until pearlite phase disappears.

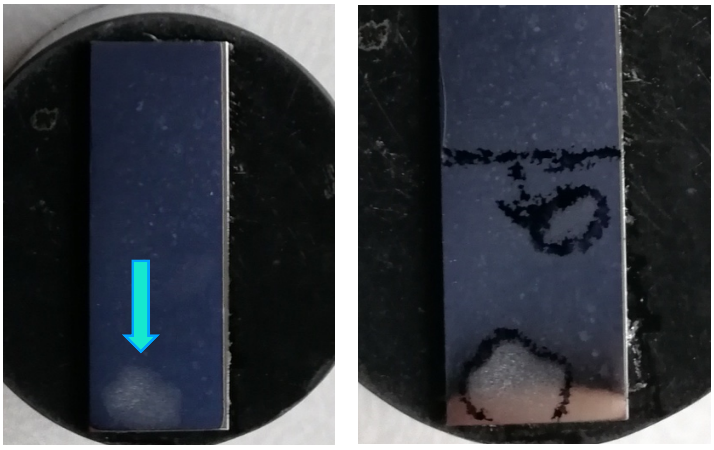

a) b)

Fig. 13. Surfaces of the sample Au2 with the bottom half covered by graphite glue. a) surface facing down during the experiment, only the relatively brighter area at the bottom had diffusion, and b) surface facing up during the experiment, carbon diffusion took place only in the two areas marked with circles. Diffusion areas of both surfaces did not match, which implies their diffusion length are lower than the thickness of the sample.

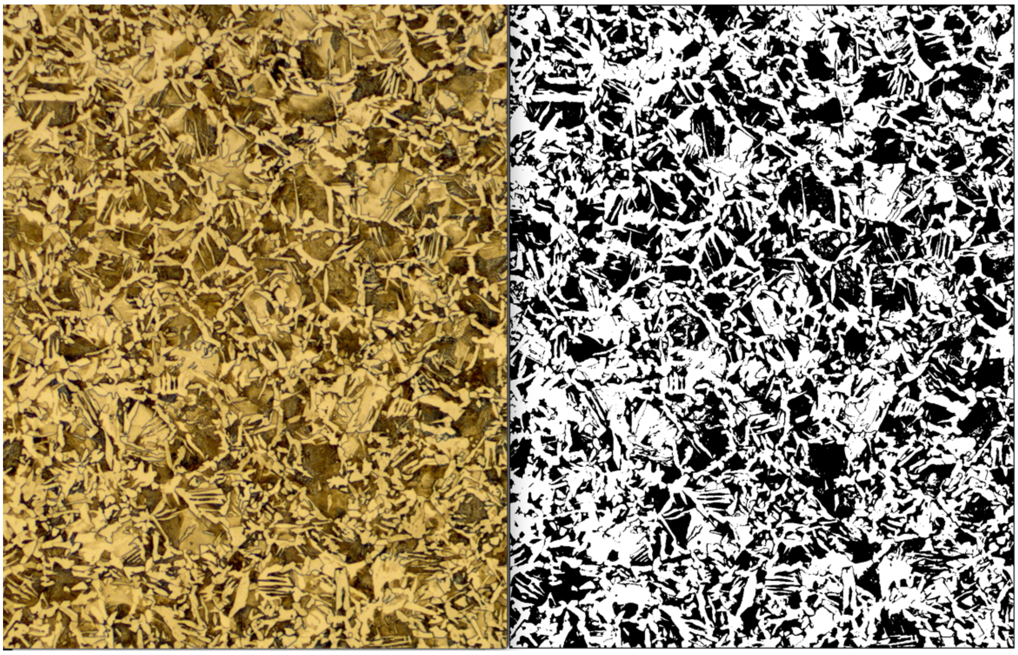

Fig. 14. Image analysis for %pearlite of the area rich in C. Left before and right after setting the threshold for area selection, 45,77% is the obtained %pearlite for this particular image.

3.2.2.3 Alumina coating

The technique involved in the alumina coating application is the one of sputtering. The technique utilizes accelerated electrons in a chamber with neutral gases to produce positively charged ion plasma. The ion plasma is then accelerated to erode the target material via energy transfer, the target material is ejected in form of neutral particles and deposed on the sample to be coated.

- Conventional oven thermal treatment

Two alumina coated samples (Al1 and Al2) with coating thickness 240nm and 980nm are put into the second level vacuum oven for thermal treatment. These samples are half-sized and they have a length of graphite glue of 0.315 inches.

Microscopic examination of the samples demonstrates the same type of microstructure as the sample without coating, see Fig. 15. The length of the area that contains pearlite phase has exceeded the length of graphite glue for 127µm for Al1 and 380µm for Al2. No significant differences appreciated between two samples.

- Thermal treatment with electric field

Two alumina-coated samples were tested in the furnace with an electric field. For sample Al4, the temperature regulation took 1h30mins approximately to reach the steady state and it remained at 875ºC for 6h 30 mins. No carbon-related microstructure was found on any of the two surfaces nor the cross-section after the thermal treatment.

For sample Al3, inhomogeneities regarding irradiance along the sample were observed during the experiment - the brightness of the sample decreases from left to right - which implies the presence of an important temperature gradient on the sample. An image of the sample was taken during the experiment, see Fig. 16b). The sample obtained from the experiment is partly molten at its upper extreme as shown in Fig. 16a), the electric current flows through the sample from the top to the bottom with the positioning shown in the figure. Similar to other alumina-coated samples, Al3 also has this blue/purple texture on its mid-section where no graphite glue was applied, meaning coating has remained on the Fe surface. A clear section reduction was visible.

The left cross-section of the sample as displayed in Fig. 16a) is being polished and Fig. 17 demonstrates the microstructure of the top area covered by graphite glue. The amount of pearlite is about to cover the cross-section of the sample and the results of image analysis are shown in Fig. 18. Though a maximum of 85% of the surface was constituted by the pearlite phase, no indications of decarburization prevention were observed by the employed metrics. The length of the area with pearlite phase is 0,329 inches and the length of the corresponding graphite glue area is 0,331 inches. This difference of 0,002 inches falls into the error that could be committing when taking measurements and is also insignificant in comparison with the expected diffusion length. On the other hand, no carbon-related microstructure was to be found on the other extreme.

Fig. 19 shows an estimation of the temperature profile of the sample. The left side of the sample has molten partly and according to the equilibrium phase diagram of Fe-C, the temperature at this area should be at around 1500ºC. On the other hand, the thermocouple welded on the middle of the sample has indicated during the experiment that the temperature was oscillating around 860ºC. Since no carbon diffusion has taken place on the right side of the sample covered by graphite glue, it is assumed to be below 700ºC which is the temperature threshold for austenite formation in Fe.

The origin of this temperature gradient could be an initial thickness inhomogeneity of the sample caused by mishandles during polishing. Given the reverse proportionality between resistance and the surface through which the electric current passes through, the part of the sample with less cross-section is subjected to higher Joule effect that heats the area to a higher temperature, as the sample slims down due to heating its resistance increases causing more heating and then the phenomenon repeats itself.

This result also hints that the location for the thermocouple may not be as appropriated to accurately determine the temperature of the sample. The indicated temperature belongs to the middle part of the sample and in the case of a temperature gradient, the parts with graphite glue may have a temperature significantly different. Given the electrodes of the device are relatively cooler than the rest of the device that are in contact with the sample, a potential explanation for not having any carbon in sample Al4 may be that the extremes of the sample are at a lower temperature, and since the thermocouple is welded in the middle of the sample, even if it is indicating the target temperature the sides could still be beneath 700ºC.

However, taking into account the results obtained from sample Au2, which had a limited diffusion area and coating detachment both of Fe and graphite glue, a possible explanation could also be that it is just the presence of electric current that is setting obstacles for C diffusion from graphite glue and it can be overcome by increasing temperatures.

The conclusions to be drawn from testing Al2O3 as coating are:

- The employed Al2O3 coating has a good attachment to Fe surface but with the tested thicknesses, no potentials have been shown to be a good decarburization-prevention coating.
- More attention should be dedicated when preparing samples since significant temperature gradients could be induced by thickness differences.
- A considerable temperature gradient could be present even the sample has a relatively homogeneous thickness, the current position of the thermocouple may not be as appropriate to indicate the temperature of the regions covered by graphite glue.
- The presence of electric current has shown once again to be preventing carbon diffusion from graphite glue to the sample and a significant increase could help overcome this obstacle.

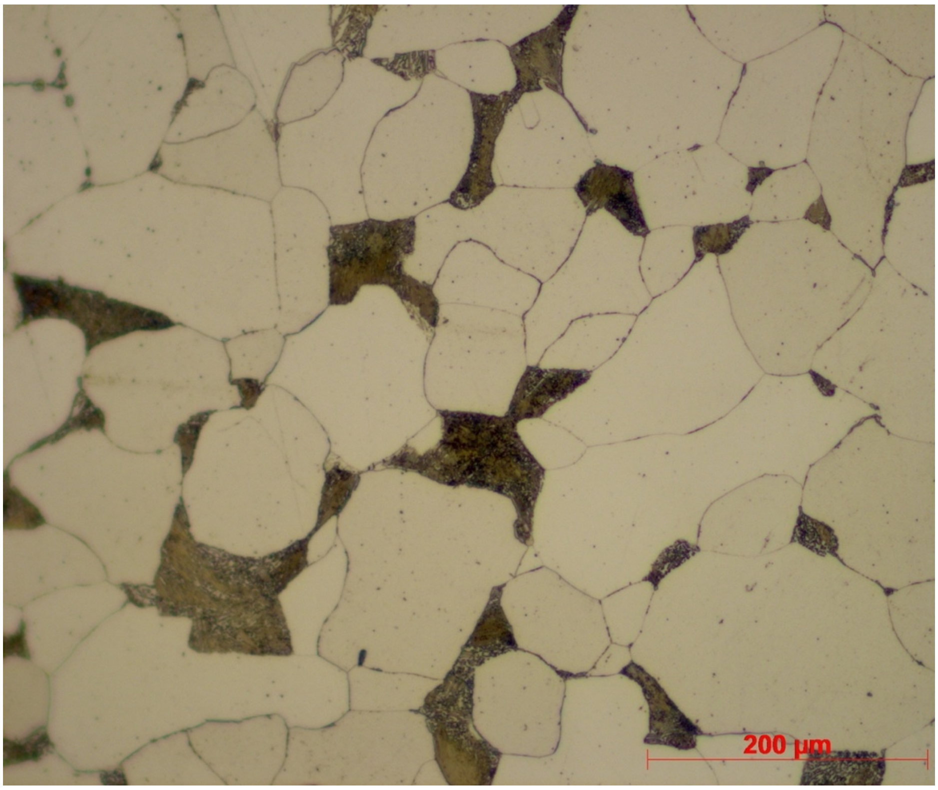

Fig. 15. Microscopic image of the half-sized sample coated with alumina, thermal treatment in conventional furnace.

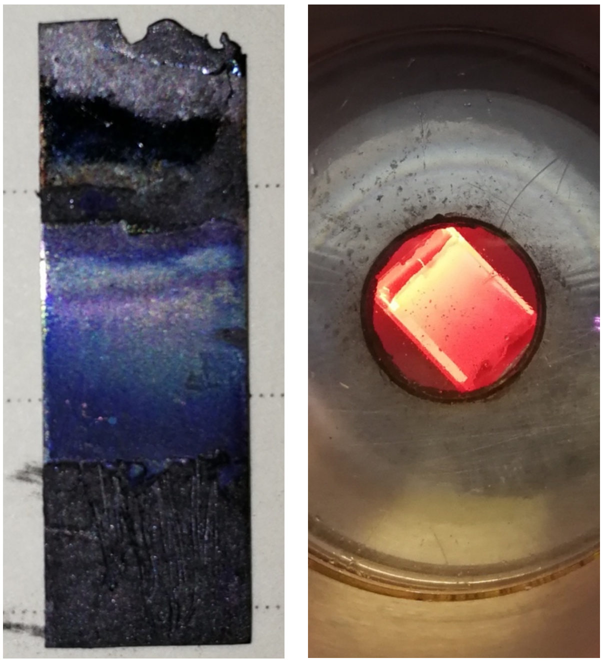

a) b)

Fig. 16. Alumina-coated sample with 240nm of thickness. a) Sample partly molten after the thermal treatment, b) Image of the sample during the experiment, temperature gradient observed along the sample.

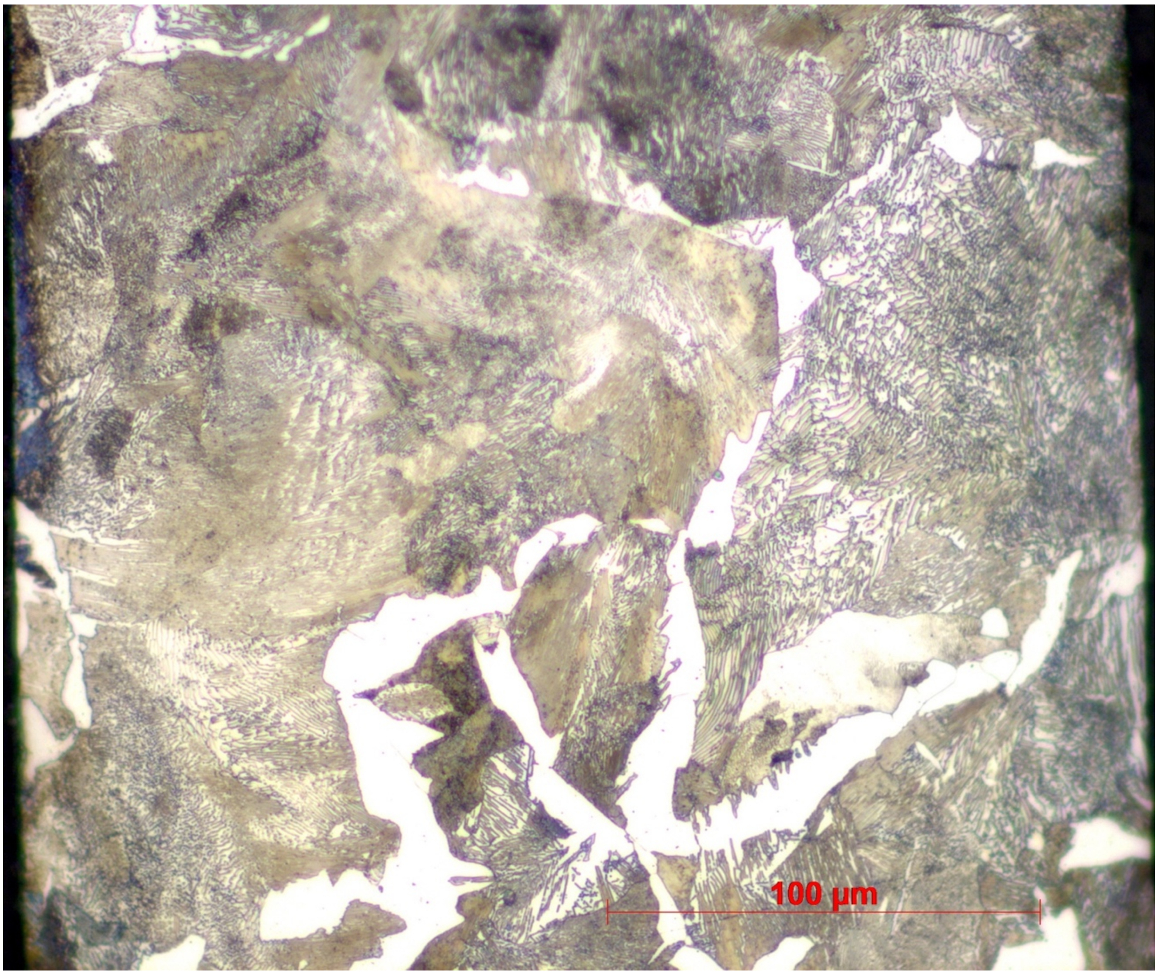

Fig. 17. Microscopic image of the sample with 240nm of alumina. A significant amount of pearlite being observed in the area covered by graphite glue.

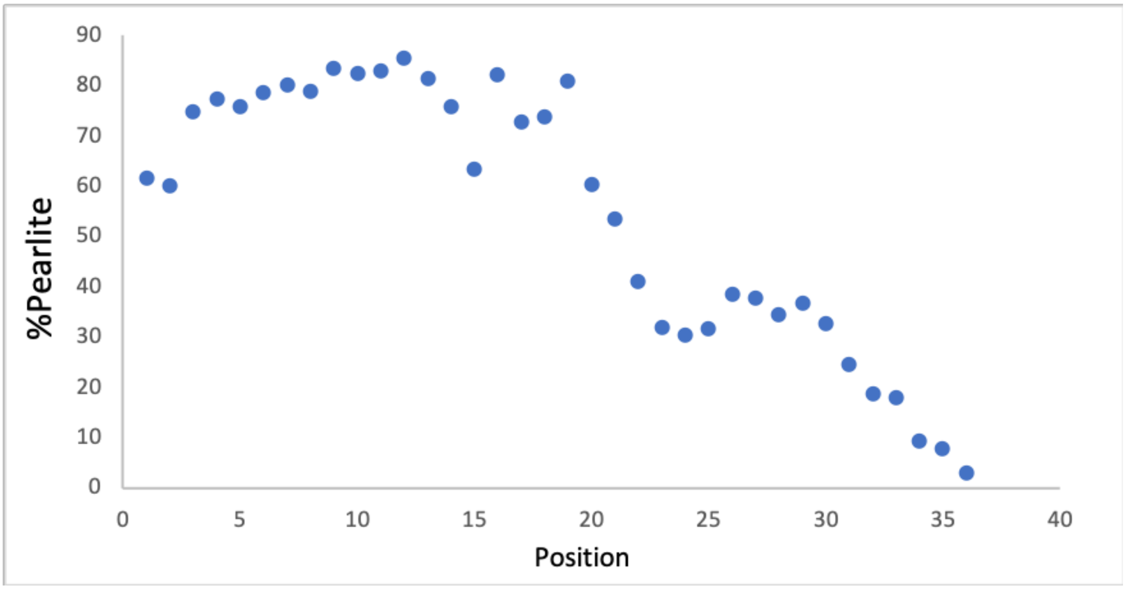

Fig. 18. Sample Al3, %pearlite vs. position from the molten going inward until pearlite phase disappears.

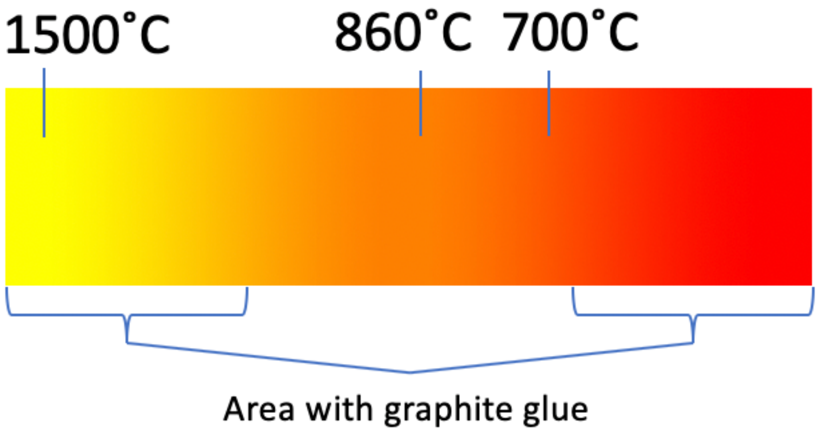

Fig. 19. Illustration of the estimated temperature distribution of the sample. Temperature decreasing from left to right.

3.2.2.4 BN coating

The polished and partly graphite-glue covered sample is sprayed with BN to obtain a homogeneous coating. The application distance is kept around 20cm to secure the coating is not excessive. The coated sample is let to dry for 15min and put into the oven at 150ºC for 15min maximizing compaction.

Four BN-coated samples had thermal treatment, being BN1 in a conventional furnace, BN2, and BN4 in a furnace with an electric field and BN3 cementation under electric and magnetic field.

- Sample without thermal treatment

Fig. 20. shows the cross-section of a sample which has neither graphite glue nor thermal treatment. The obtained coating has a thickness between 50 to 150µm, it covers the entire sample and seemingly well attached.

- BN1, sample with thermal treatment in the conventional furnace

Sample BN1 had a conventional heat treatment and quenched in water right after the experiment. The presence of C diffusion is observed under microscope and its microstructure is well different in comparison with the ones obtained from the same heat treatment. A microstructure image of the sample BN1 is shown in Fig. 21. Unlike the clear alternating-layer structure of pearlite phase observed in NC, BN1 has a more martensite-like microstructure due to the lack of carbon diffusion caused by quenching.

- Samples with thermal treatment with electric field/cementation with an electromagnetic field

Samples BN2, 3, and 4 have a different arrangement when it comes to graphite glue application (see Fig. 22). The area applied with graphite glue is limited in one section on the top surface of the sample, as shown in the figure. The testing with an electric field of the sample Al4 showed no presence of C and one potential explanation is that the fact that the electrodes of the setup are at a lower temperature, it may have induced a temperature gradient and with the thermocouple being welded in the middle, the distance between the thermocouple and the area covered by graphite glue may cause a temperature measurement not as precise as desired.

BN coatings are incomplete after thermal treatments with small areas without BN coating throughout the Fe surface. For sample BN2, neither of the surfaces demonstrated any presence of carbon - the diffusion of carbon atoms from the graphite glue did not take place as pretended.

During the experiment of sample BN3, the surface covered by graphite glue presented inhomogeneities regarding irradiance. The texture of the area covered by graphite glue is not homogeneous after its heat treatment, some regions were darker than the rest, see Fig. 23. The sample after thermal treatment is no longer flat but slightly bent along its diagonal. Both surfaces were polished and etched for microscopical observation, as well as its right cross-section with the sample placed as shown in Fig. 23. The two areas pointed by arrows in Fig. 23 are more prominent in comparison with the rest of the surface, C diffusion only took place in these two regions.

Fig. 24a) and b) demonstrate images of the upper surface of BN3 captured by an optical microscope. Fig. 24a) shows the small region close to its left edge and Fig. 24b) close to its right edge where the presence of pearlite was found. No C diffusion observed on the opposite surface.

The temperature at the steady state of the experiment was set to around 920ºC and it has remained at this temperature for about 4 hours, it took 1h20mins to reach the target temperature.

Sample BN4 was also tested with thermal treatment under electric filed since pearlite was observed in BN3, the goal was to redo the experiment expecting a different result so conclusion regarding the influence of magnetic field could be drawn. It was intended to mimic the experimental conditions of BN3: the experiment lasted 4h45mins, it took 45mins for the sample to reach 870ºC and the temperature was intentionally lowered to 860ºC until around 1h20mins when the thermocouple of the sample stopped working. The temperature of the heating resistance was raised up to 1220 so the temperature of the sample could be estimated to be around 925ºC for the rest of the experiment.

Part of the graphite glue was being detached from the sample during the thermal treatment and the microscopical observation on neither the surface nor the cross-section of the sample revealed any indications of carbon diffusion.

Conclusions:

- Similar to other employed coatings, BN-coated samples haven't shown either the C diffusion profile as a sample without decarburization.
- Samples BN2 and BN4 are tested in the furnace with electric field and no C diffusion was observed, just as in the cases for Au2 and Al4. Once again it has proven that C diffusion from the employed graphite glue can be prevented by the electric current with the described experimental conditions.
- The application of a high-intensity magnetic field with its direction perpendicular to the surface of the sample can seemingly help overcome the barrier set by the electric field, however, given the limited sample size, this conclusion is too early to be drawn.

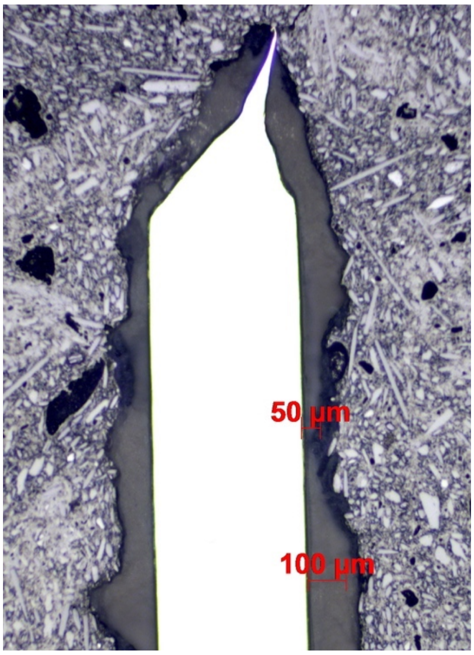

Fig. 20. Pure iron sample covered by BN.

Fig. 21. Martensite-like microstructure of sample BN1.

Fig. 22. Illustration for samples BN2, 3, and 4.

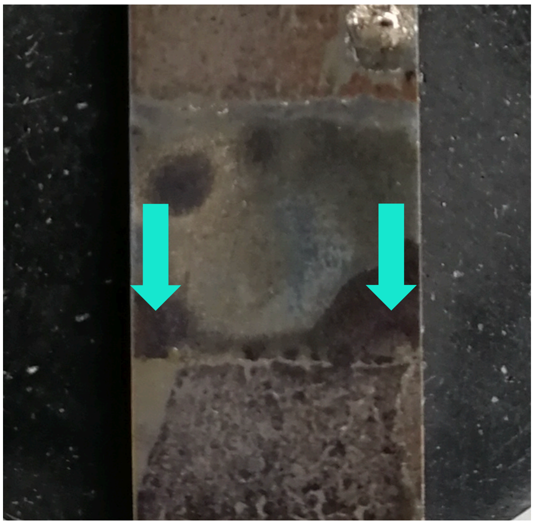

Fig. 23. Picture of sample BN3 after the thermal treatment. The section in the middle belongs to the area covered by graphite glue where an area clearly darker than the rest is appreciated. Only the areas pointed by arrow had C diffusion.

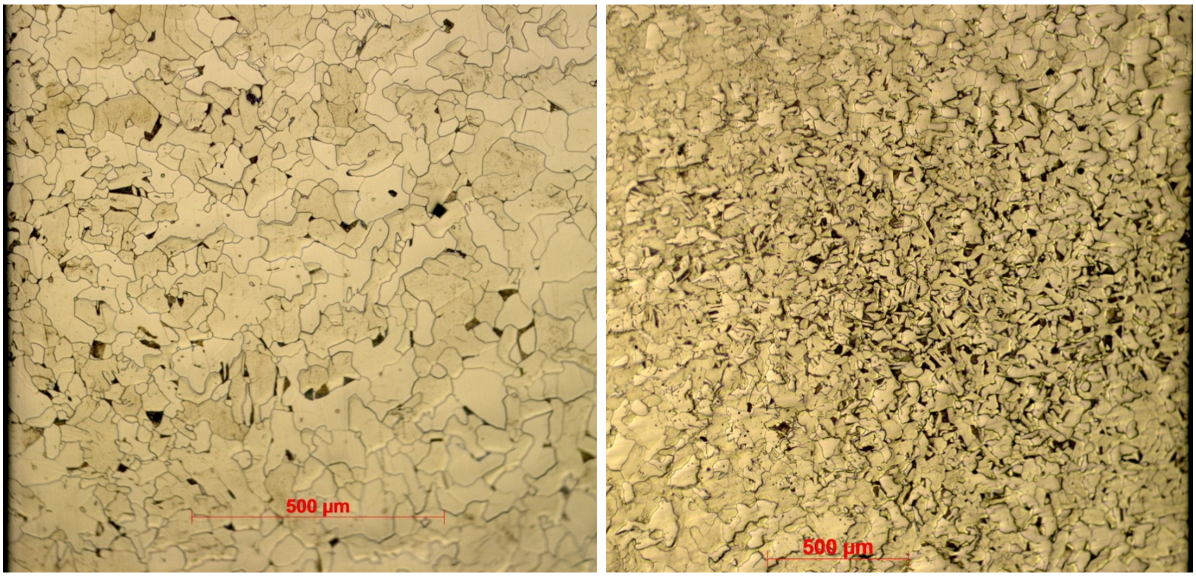

a) b)

Fig. 24. Areas of sample BN3 that had C diffusion. a) Area close to its left edge and b) right edge.

4. Conclusion

During the elaboration of this work, samples were coated by different materials with the intention of finding a means to prevent decarburization. Au, Al2O3, and BN are applied as coatings to the samples with their owned methods and are tested in ovens with and without an electric field. The obtained results are then compared to the ones suggested by theoretical understanding and results from previous experiments. A sample without the application of any coating was tested so its microstructure could be used to compare with the ones obtained from samples with coatings.

None of the three employed coatings had the ability to provide results expected from a sample that does not experience decarburization. C diffusion profiles are observed and compared and relative lengths of diffusion are measured as means of testimony.

For samples coated with Au, a problem of attachment with the Fe surface was constant in all two experiments and the same problem with the graphite glue surface was seen when having thermal treatment with an electric field. BN samples have neither stayed entirely on the surface of the sample during the testing. The presence of an electric field has the effect of preventing C diffusion from graphite glue to the sample since not carbon-related phases were present in neither Al2O3 nor BN coated samples tested with furnace plus electric field. The presence of Au coating, a magnetic field with the described conditions or higher temperature can seemingly counteract this phenomenon.

The results provided by the experiment of sample Al3 revealed the importance of sample thickness homogeneity for the experiment with the electric field given its impact on the homogeneity of Joule effect that the setup can provide with.

5. References

[1] P. Chantrenne, D. Fabrègue, M. Perez, *et al*. Cementation Assisted by Electric Current.
[2] Wang S, Wu Y, Zhao X, Zuo L. Effect of a High Magnetic Field on Carbon Diffusion in γ-Iron. *Mat. Trans.* **139-141** (2011), 52.
[3] Wang X, Wei L, Zhou X, *et al*. A superficial coating to improve oxidation and decarburization resistance of bearing steel at high temperature. *Applied Surface Science,* **4988-4982** (2012), 258.
[4] Wang X, Wei L, Zhou X, *et al.* Protective Bauxite-Based Coatings and Their Anti-decarburization Performance in Spring Steel at High Temperatures. **753-758** (2013), 22.
[5] W. Ernst, J. Neidhardt, H. Willmann, *et al*. Thermal decomposition routes of CrN hard coatings synthesized by reactive arc evaporation and magnetron sputtering. *Thin Solid Films,* **568-574** (2008), 517.
[6] Matthew A Steiner (2014) Strain-Induced Microstructural and Ordering Behaviours of Epitaxial Fe38.5Pd61.5 Films Grown by Pulsed Laser Deposition (Doctoral dissertation). Retrieved from Research Gate.
[7] Julia V. Lyubina (2007) Nanocrystalline Fe-Pt Alloys: Phase Transformations, Structure and Magnetism (Doctoral dissertation). Retrieved from Research Gate.

6. Appendix

Detailed information regarding the compositions of the coatings from the literature research.

Details on the composition of the coating number 1, found in literature research.
Tables 1 and 2 shows the composition of its constituent parts, dolomite and bauxite, and table 3 shows the composition of the coating.

Component	MgO	CaO	SiO2	Fe2O3	Al2O3
Content [wt. %]	39.92	58.72	0.64	0.46	0.36

Table 1. [3] Composition of the dolomite.

Component	Al2O3	SiO2	TiO2	Fe2O3	CaO	K2O
Content [wt. %]	63.96	29.15	3.36	2.41	0.76	0.36

Table 2. [3] Composition of the bauxite.

Component	Dolomite	Silicon carbide	Bauxite	Citric acid	Distilled water
Parts by weight	64	20	20	7	29

Table 3. [3] Composition of the coating.

Component	C	Cr	Mn	Si	S	P	Fe
Content [wt. %]	1	1.5	0.3	0.25	0.01	0.01	96.93

Table 4. [3] Composition of the bearing steel.

Details on the composition of the coating number 2, found in literature research.
Tables 4 and 5 show the composition of the bauxite and the coating powder used for this coating.

Component	Al2O3	SiO2	TiO2	Fe2O3	CaO	K2O	P2O5	ZrO2	MgO
Content [wt. %]	75.17	15.99	4.34	3.28	0.32	0.31	0.28	0.21	0.10

Table 5. [4] Composition of the bauxite.

Component	SiC	Al2O3	SiO2	TiO2	Fe2O3	CaO	K2O	P2O5	ZrO2	MgO
Content [wt. %]	42.86	42.95	9.14	2.48	1.87	0.18	0.18	0.16	0.12	0.06

Table 6. [4] Composition of the coating powder.